Neurodevelopment, brain vasculature and schizophrenia

Puvogel Lütjens, Sofía

DOI:
10.33612/diss.582204366

Chapter 2

Single-nucleus RNA sequencing of the adult human subependymal zone reveals a decline in the relative abundance of oligo progenitors and transcriptional changes in different cell types associated with age

Sofía Puvogel[1,2], Astrid Alsema[2], Maree J. Webster[3], Cynthia Shannon Weickert[4,5,6], Bart J.L. Eggen[2]

[1] Department of Biomedical Sciences of Cells and Systems, section Cognitive Neuroscience, University of Groningen, University Medical Center Groningen, Groningen, The Netherlands.
[2] Department of Biomedical Sciences of Cells and Systems, section Molecular Neurobiology, University of Groningen, University Medical Center Groningen, Groningen, The Netherlands.
[3] Laboratory of Brain Research, Stanley Medical Research Institute, Rockville, MD, USA.
[4] Schizophrenia Research Laboratory, Neuroscience Research Australia, Sydney, NSW, Australia.
[5] School of Psychiatry, University of New South Wales, Sydney, NSW, Australia.
[6] Department of Neuroscience and Physiology, Upstate Medical University, Syracuse, NY, USA.

Manuscript in preparation

Abstract

The subependymal zone (SEZ), also known as the subventricular zone, constitutes a neurogenic niche that persists during post-natal life. In humans, the neurogenic potential of the SEZ declines with age, however studies have highlighted the relevance of the cellular niche and the neurogenic capacity of the neuronal progenitors in the adult human SEZ, and have identified neurogenic activity during adulthood under particular conditions. In the present study, the complete cellular niche of the adult human SEZ was characterized by single-nucleus RNA sequencing (4 young and 4 middle-aged adults). While different cellular clusters expressing neural stem cells (NSCs) marker genes were identified, none expressed proliferation-related genes, suggesting that the NSCs of the adult SEZ are in a quiescent state. The relative abundance of NSC clusters did not differ between the two age groups, indicating that the pool of SEZ NSCs does not decline in this age range. The expression of genes related to nervous system development was higher across different cell types, including NSCs, in young adults as compared to the middle-aged group. These transcriptional changes suggest ongoing central nervous system development in early adulthood, which may decline in middle age. The relative abundance of oligodendrocyte progenitors also decreased in middle-age, indicating that the cellular composition of human SEZ is remodeled between early and middle adulthood.

Introduction

The subependymal zone (SEZ), also known as the subventricular zone, lines the walls of the lateral ventricles and constitutes a neurogenic niche that remains active during post-natal life [1]. In humans, neurogenic activity decreases one year after birth and may be lost by adulthood [2, 3]. While some studies provide evidence for proliferating cells in the adult human SEZ [4-6], there is debate as to whether these proliferative signals derive from neural stem cells (NSC) that give rise to neuronal progenitors [7]. In addition, there is evidence indicating that the majority of NSCs in the adult human SEZ are in a quiescence state [3, 8], and can be reactivated under certain conditions, governed by environmental and niche derived factors [9-12]. Transcriptional characterization of the different cell types that comprise the adult human SEZ may answer whether there is active neurogenesis in the adult SEZ. Furthermore, if the cellular niche of the adult NSCs modulates their neurogenic potential, then a better understanding of the SEZ cellular heterogeneity during adulthood will provide clues as to what may influence its neurogenic capacity.

In general, the fate of NSCs is modulated by their cellular niche. Signals derived from the niche in the form of soluble factors or cell-cell contacts can induce NSCs to self-renew or differentiate. For instance, β-catenin produced by endothelial cells promotes NSCs proliferation [13], while retinoic acid secreted by astrocytes promotes differentiation [14]. Variations in the neurogenic capacity of the adult SEZ have been observed under some pathological conditions that may disrupt the SEZ cellular niche. For example, PCNA positive cells (a marker of cell proliferation) that co-stained with neuronal or astrocytic marker genes were observed in *post-mortem* SEZ tissue of patients with Huntington's [9], a neurodegenerative disease that severely affects the caudate nucleus, adjacent to the SEZ. Conversely, very few PCNA positive cells were detected in tissue from control donors. In Parkinson's patients, deep brain stimulation (DBS) near the SEZ increased the number of PCNA positive cells that co-expressed δ-GFAP, a NSCs marker gene [15], as compared to control tissue from donors without DBS. While ischemic injury and epilepsy increase the number proliferative cells in the human SEZ [16, 17], aging seems to negatively affect proliferation in the human SEZ, as reflected by a decrease in expression of NSCs and cell cycle-related genes in aged tissue [5, 18]. The neurogenic potential of the adult human SEZ may be influenced by

signals derived from different cell types, but the cellular diversity of this highly specialized niche has not been resolved, and is therefore the focus of this study.

Single-cell or nucleus RNA sequencing (sc/snRNAseq) enables transcriptional profiling at single-cell resolution [19], and provides information about the transcriptional heterogeneity of all the different cell types in a tissue. The mouse SEZ has been extensively studied with single cell transcriptomics [20-24], but only one study using snRNAseq of the adult human SEZ has been published [8]. To sequence a higher proportion of potential SEZ progenitor cells, Donega et al., 2020 [8] sorted and sequenced CD217 positive cells. However, with this enrichment technique they primarily sequenced oligodendrocytes and oligo progenitors, and probably missed most other cell types. In addition, they only included donors over 70 years old; therefore, changes associated with age across the different cell types in the adult human SEZ have yet to be explored.

In the present study, we used snRNAseq to reveal the transcriptional heterogeneity and relative abundance of all the different cell types that comprise the adult human SEZ. We included 4 young adults (Y-ad; average age of 20) and 4 middle-aged adults (M-ag; average age of 50), to evaluate whether the cellular composition and the transcriptomic profile of the human SEZ differs between early and middle adulthood. These data serve as a starting point to identify and characterize the cell types with potential stem cells features in the adult human SEZ, and to investigate the effect of age on this cellular niche.

Materials and Methods

Human brain tissue and nuclei isolation

Lateral ventricular subependymal zone (SEZ) samples from 4 young adults (Y-ad; average age=20) and 4 middle-aged adults (M-ag; average age=50) were obtained from the Stanley Medical Research Institute (SMRI) (S. Table 1). *Post-mortem* brains were obtained from Medical Examiners with the permission from the next-of-kin. Ethical approval for the brain collection was through the Uniformed Services University for Health Sciences, Bethesda, MD. A crysostat was used to cut seven, 100um thick, coronal sections from fresh frozen blocks of caudate nucleus. The SEZ tissue was dissected from each section, ~2mm deep to the surface of the lateral ventricle. To ensure the quality of the brain tissue, RNA was isolated using RNeasy Lipid Tissue mini kit (Qiagen, 74804) and RNA concentration and integrity were measured on a Bioanalyzer 2100 (Aligent). The average RIN value of the samples was 8, and all presented a RIN > 7 (S. Table 1). Nuclei were isolated from the SEZ samples, as described in [25]. After sucrose density centrifugation, ~ 40,000 DAPI positive events were sorted per sample and subjected to snRNAseq.

Demographics

The two age groups (Y-ad and M-ag) were matched for quantitative variables (S. Table 1). A parametric (Student's t-test) or a non-parametric test (Mann-Whitney U test) was used, depending on the data distribution, to show the two groups were not statistically different for any of the case-related variables (S. Table 2), except for age.

Immunohistochemistry

Paraffin embedded (10um), or fresh frozen (14um) coronal sections through the caudate nucleus were stained with polyclonal antibody to JUND (ThermoScientific, #720035) or monoclonal antibody to PCSK1N (LifeSpan Biosciences, LS-C134062). Fresh frozen sections were thawed and fixed with 4% paraformaldehyde before the primary antibody was applied (1:200) overnight at 40C. Paraffin sections were incubated in 90 C bath of 0.01M citrate buffer for 30 mins before the primary antibody was applied (1:200) overnight at 40C. Following washes, sections were incubated in biotinylated secondary antibody (1:100), washed and incubated with avidin-biotin-

peroxidase complex (Vectastain ABC kit, Vector Laboratories, Burlington, CA), treated with 3,3'-Diaminobenzide, washed, stained with Nissl and coverslipped.

snRNAseq library construction and sequencing

Single nucleus cDNA libraries were constructed according to the user guide of Chromium Single Cell 3' Reagents Kit v3.1 (10x Genomics). All samples were pooled in equimolar ratios and sequenced on a NextSeq 500 at the Research Sequencing Facility of the UMCG, Groningen, The Netherlands. The median sequencing depth was 122 million reads per sample and the median counts per nuclei was 2,614.

snRNAseq data analysis

Sequencing reads were processed and aligned to the GRCh38 human genome using CellRanger v3.0.1 [26]. Filtered count matrices generated by Cell Ranger were loaded in R v4.0 with Seurat v4.0 [27]. Nuclei with mitochondrial content > 5% were removed. Count information of the 8 cases was LogNormalized and integrated according to guidelines for fast integration with reciprocal PCA (rPCA) in Seurat. Integrated data were scaled using *ScaleData* function and regressing on "nCount_RNA", "percent.mito", "percent.ribo", and "nFeature_RNA". Scrublet v0.2.1 was used to remove doublets. After these pre-processing steps, 36,626 nuclei were retained, with 5,037 reads per nuclei on average. Unbiased clustering analysis followed by examination of marker gene expression was performed to identify all major SEZ cell types. *FindAllMarkers* function from Seurat v4.0 with default parameters was used to identify only positive differentially expressed genes per cluster (marker genes). Marker genes per cluster are provided in S. Table 3.

Hierarchical clustering

A Person's correlation matrix was calculated on the average transcriptomic profiles of the clusters, considering only highly variables genes. The correlation matrix was used as an argument for *heatmaply* function of Heatmaply R package v1.3.0 [28], specifying hclust_method=NA to automatically determine the optimal dendrogram for the data.

Gene ontology enrichment analysis

Gene ontology (GO) enrichment analysis was performed on the abundantly expressed genes of each cluster ($log_2FC > 0.5$ and adjusted p value <0.05), using the *gost* function of the R package gprofiler2 v0.2.1. *P* values were adjusted for multiple

comparisons setting correction_method=g_SCS. Redundancy of enriched biological processes GO terms was accounted for with clustering analysis and aggregating terms with high semantic similarity using the functions *calculateSimMatrix*, setting ont="BP", and *reduceSimMatrix* with threshold=0.7 of the rrvgo v1.2.0 R package.

Characterization of clusters expressing neuronal and neural stem cells marker genes

Clusters expressing neuronal and/or NSCs marker genes (clusters 16, 0, 7, 8, 19, 11, 13, 14, 2, 3, 12, 10 and 9) were extracted from the dataset. Count information of these nuclei was re-integrated across the samples using canonical correlation based integration. Downstream pseudotime and enrichment analyses, detailed below, were performed on this nuclei subset.

Pseudotime analysis: A pseudotime trajectory was calculated through the transcriptomic profiles of the nuclei subset, following the guidelines of the R package Destiny v3.4.0 [29]. Briefly, count data of highly variable genes within the nuclei subset were used to identify the diffusion components with *DiffusionMap*, using default parameters. *DPT* function was used to calculate the pseudotime trajectory and *random_root* parameter was activated to automatically identify the source nucleus of the trajectory. To identify the most relevant driver genes of the pseudotime trajectory, we used *gene_relevance* [30] with dims=1:3.

Enrichment of marker genes of mouse SEZ cell types: We used *AddModuleScore* function of Seurat, with default parameters, to evaluate the enrichment of gene sets associated with mouse SEZ cell types in our human SEZ clusters.

Enrichment of neurodevelopmental diseases associated genes: The R package MAGMA.Celltyping v2.0.1 with linear enrichment mode [31, 32] was used in R v4.1 to evaluate whether genes previously associated with different neurodevelopmental diseases were specifically expressed by any SEZ neuronal and/or NSCs cluster. LogNormalized data of the variables genes within the nuclei subset were used to generate a CellTypeData (CTD) file, with *generate_celltype_data* function. *load_rdata* from EWCE v1.3.3 [33] was used to load the generated CTD in R. The genes associated with schizophrenia [34], bipolar disorder [35], autism [36] and Chron's disease [37] were obtained with *import_magma_files* function, setting ids=c("ieu-a-22", "ieu-b-41", "ieu-a-1185", "ieu-a-12"). With *celltype_association_pipeline*, we estimated

the enrichment of genes associated with the mentioned diseases in our subset of neuronal and NSCs clusters, setting ctd_species="human" and run_linear=TRUE.

Group comparisons

We compared the age groups in terms of the transcriptomic profiles and relative abundance of the different clusters.

Identification of differentially expressed genes between Y-ad and M-ag: To test for differences in the transcriptomic profiles of the SEZ clusters between Y-ad and M-ag, we made a prior selection of genes per cluster that met the following conditions: **1)** expressed in at least 25% of the nuclei in one of the two age groups, **2)** with absolute $\log_2$FC > 0.25 between the two groups. Only expression data derived from samples that contributed more than three nuclei to the given cluster were considered. The *zlm* function of the R package MAST v1.16.0 [38] was used to identify the differentially expressed genes (DEGs) between Y-ad and M-ag in each cluster. We corrected gene expression by the cellular detection rate and included a random intercept per case to account for donor-related structure in the data. The results of this analysis are provided in S. Table 4. After corrections, genes were considered differentially expressed when the effect of age had a log2 fold change > 0.1, with a false discovery rate (FDR) adjusted *p* value < 0.05.

Comparison of clusters proportions between Y-ad and M-ag: A generalized linear model (GLM) was used to test if age (Y-ad or M-ag) affects the probability of a nucleus belonging to a given cluster. We used the *glmer* function of the lme4 R package v1.1.27.1 [39] with a quasibinomial distribution, because of the binary nature of the response variable (the nucleus either belongs to the given cluster or not). Considering that a model was created per cluster, the obtained *p* values were corrected with the Bonferroni method and the number of comparisons was set to the total number of clusters.

Estimation of clusters proportions in bulk transcriptomic data: "Impute Cell fractions" method of CIBERSORTx software [40] was used to estimate the proportion of our SEZ snRNAseq clusters in bulk transcriptomic data from SEZ samples of 20 donors, aged from 15 to 86 years old [18]. These donors were previously assigned to 4 different age groups, adolescents (average age=15.5 years), young adults (average age=23 years), adults (average age=42.3 years) and aging (average age=86 years)

[18]. The signature matrix, reflecting the average transcriptomic profiles per SEZ snRNAseq cluster, was generated using count data of the highly variable genes. The mixture file was generated with the bulk RNA sequencing data [18]. Counts of each expressed gene were divided by the total number of counts in each sample and multiplied by 1,000,000 (CPM normalization). To corroborate the differences in the relative abundance of SEZ clusters associated with age, identified in the snRNAseq dataset, we compared the estimated proportion in the bulk RNA sequencing data, obtained with CIBERSORTx, of cluster 4 (oligo progenitors), cluster 6 (microglia) and cluster 13 (neuronal cluster) between the 4 different age groups. We used a Kruskal Wallis test and post hoc analysis was performed with Dunn Test. *P* values were FDR corrected.

Results

Single-nucleus RNA sequencing and cellular composition of the adult human SEZ

Nuclei were isolated from SEZ samples of 4 young and 4 middle-aged adults (Y-ad, M-ag; Figure 1 A.I). DAPI positive events were sorted and subjected to snRNA sequencing (Figure 1 A.II). Unbiased cluster analysis of nuclear transcriptomic profiles of 36,626 nuclei revealed 20 clusters (Figure 1 B). To identify the major brain cell types, clusters with similar transcriptomic profiles were grouped together, based on hierarchical clustering analysis (Figure 1 C, top), and annotated into 11 different main cell types, based on the expression of cell type-specific marker genes (Figure 1 C, bottom) and gene ontology enrichment analysis (Figure 1 D).

The first three clusters ordered from left to right in the dendrogram (clusters 16, 0 7, Figure 1 C), were enriched for genes expressed by neuronal progenitor or NSCs, such as *ID4* [41, 42], *SOX2* [43], and *SOX5* [44, 45], as well as astrocyte marker genes, such as *SLC1A3* and *AQP4* [46]. Cluster 0 was the only one of these three clusters that highly expressed *HES5*, involved in maintenance of the undifferentiated state in neuronal progenitor cells [47], while both clusters 0 and 16 abundantly expressed *GLI3*, a transcription factor activated through Sonic Hedgehog signaling and required to maintain mouse neural progenitors actively in the cell cycle [48]. Additionally, clusters 0 and 16 highly expressed *LFNG*, a Notch receptor modifier that is expressed in adult mouse NSCs, regulating their cycling [49]. Cluster 0 together with cluster 7 highly expressed *PAX6*, which modulates NSCs differentiation [50, 51]. In each of these three clusters, the most enriched gene ontology biological term was associated with development (Figure 1 D). Since clusters 16, 0 and 7 exhibited a transcriptomic profile related to both astrocytes and neural progenitors (or stem cells), we annotated them as Astro/NSCs, and the three together represented 19.3% of the SEZ cell types (Figure 1 E).

The nuclei in cluster 8 were annotated as ependymal, because of their high expression of Doublecortin Domain-Containing Protein 1 (*DCDC1*) and *FOXJ1*, both marker genes of ependymal cells [52]. Ependymal nuclei corresponded to 3.1% of SEZ cell types. Interestingly, ependymal cluster also highly expressed the stem cell marker genes *ID4*, *SOX2*, and *SOX9* [53], suggesting potential stem cells features in SEZ ependymal

cells. Cluster 4 was annotated as oligo progenitor cells (OPCs), based on the expression of OPCs marker genes such as *VCAN*, *PCDH15*, and *MEGF11* [54, 55], and represented 8.1% of the SEZ cell types.

We identified 8 clusters of neurons (19, 11, 13, 14, 2, 3, 12, 10). Cluster 19 was annotated as somatostatinergic neurons (SST neurons), based on its high *SST* expression activity. All the other neuronal clusters highly expressed *GAD2*, suggesting that these nuclei derived from GABAergic inhibitory neurons.

Although clusters 11, 13, 14 exhibited high *RBFOX3* expression, which is typically expressed by post-mitotic neurons [56], they abundantly expressed *DLX6-AS1*, which is expressed in neuronal progenitor cells [57]. Additionally, clusters 11 and 13 highly expressed *EGFR*, also expressed by neuronal progenitors and relevant for their survival and proliferation [58, 59]. Cluster 11, the cluster with highest *DLX6-AS1* expression activity (Table 3), also highly expressed *PDGFD*, which is expressed by human radial glia cells in the ventricular zone during corticogenesis [60]. The expression of progenitor marker genes in neuronal clusters 11, 13 and 14 may suggest that these clusters correspond to immature neurons, or to neurons that became post-mitotic more recently as compared to other neuronal clusters. Clusters 11, 13 and 14 were annotated as DLX6-AS1 neurons, and together represented 3.7 % of the identified cell types in the human SEZ (Figure 1 E).

We identified four clusters of medium spiny neurons (clusters 2, 3, 12 and 10; MSPNs), which probably derived from the adjacent striatum, based on their high expression of *BCL11B* [61]. It was previously described for mouse that MSPNs adjacent to the SEZ express either dopamine receptor 1 or 2 [20]. In our human data set, MSPNs clusters 2 and 10 highly expressed *DRD1*, while *DRD2* was expressed by MSPNs cluster 3 and 12. Altogether, the MSPNs clusters represented 26.6 % of the cell types.

The next cluster in the dendrogram, cluster 9, did not express *RBFOX3* but expressed other genes previously described as highly expressed in neurons, such as NMDA glutamate receptor Subunit 1 (*GRIN1*) and the gene coding for Calycon (*CALY*) [62]. Nonetheless, nuclei in cluster 9 also abundantly expressed genes that were previously identified as highly expressed by neuroblasts in the adult mouse hippocampal neurogenic niche, such as *TMSB10* and *NNAT* [63]. The top enriched term in cluster 9 abundantly expressed genes was cytoplasmic translation (Figure 1 D). Interestingly,

mouse SEZ neuroblasts and active NSCs (aNSCs) highly express ribosomal and translation related genes too [21, 24], suggesting that cluster 9 may share some features with neuroblasts and/or aNSCs. Cluster 9 was annotated as high-translation and represented 9.2% of the cell types in human SEZ.

Nuclei of cluster 15 highly expressed marker genes of endothelial cells, such as *CLDN5*, as well as pericytes and smooth muscle cell marker genes, such *DLC1* and *TAGLN*, respectively (Figure 1 C) [64]. “Blood vessel development” was the most enriched biological term in the highly expressed genes of cluster 15 (Figure 1D). Together, these results indicate that this cluster contained a mixture of nuclei derived from different brain vascular cells and represented 1% of the identified SEZ cell types (Figure 1 E). Cluster 18 corresponded to lymphocyte nuclei (0.2% of the cell types) that abundantly expressed *IL7R* and *SKAP1* [65, 66]. The top enriched term in cluster 18 was T cell activation. Cluster 6 contained microglia nuclei, enriched for *P2RY12* and *CX3CR1* [65, 67]. Microglia accounted for 6.7 % of the SEZ cell types. Clusters 17, 1 and 5, highly expressed the myelin associated oligodendrocyte basic protein (*MOBP*) gene and were identified as oligodendrocytes. Together, the three oligodendrocytes clusters represented 22% of the cell types.

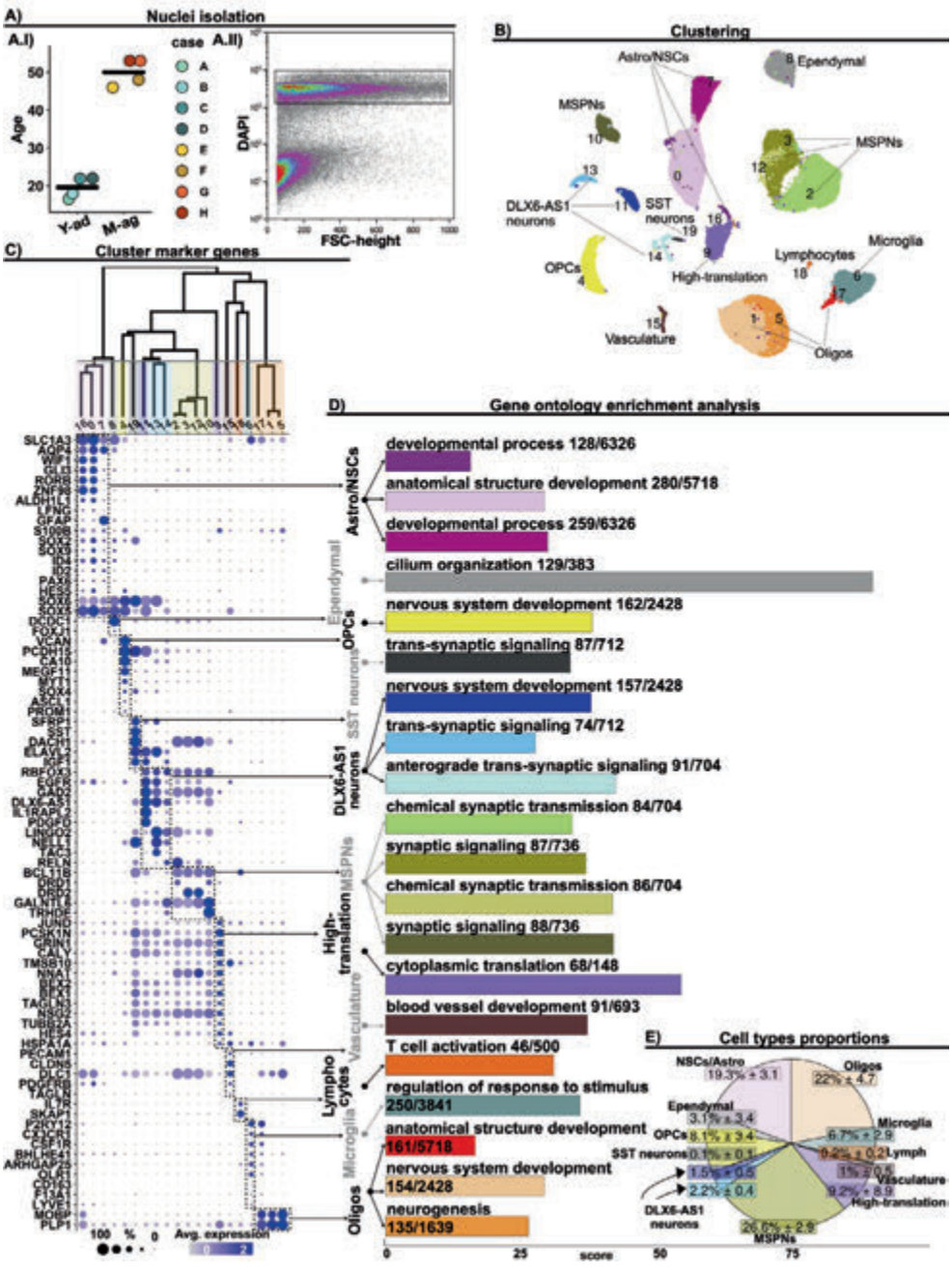
A)
Nuclei isolation
A.I)
A.II)
case
Age
Y-ad
M-ag
DAPI
FSC-height
B)
Clustering
Astro/NSCs
Ependymal
MSPNs
DLX6-AS1 neurons
SST neurons
OPCs
High-translation
Lymphocytes
Microglia
Vasculature
Oligos
C)
Cluster marker genes
Avg. expression
D)
Gene ontology enrichment analysis
developmental process 128/6326
anatomical structure development 280/5718
developmental process 259/6326
cilium organization 129/383
nervous system development 162/2428
trans-synaptic signaling 87/712
nervous system development 157/2428
trans-synaptic signaling 74/712
anterograde trans-synaptic signaling 91/704
chemical synaptic transmission 84/704
synaptic signaling 87/736
chemical synaptic transmission 86/704
synaptic signaling 88/736
cytoplasmic translation 68/148
blood vessel development 91/693
T cell activation 46/500
regulation of response to stimulus 250/3841
anatomical structure development 161/5718
nervous system development 154/2428
neurogenesis 135/1639
score
E)
Cell types proportions
NSCs/Astro 19.3% ± 3.1
Oligos 22% ± 4.7
Ependymal 3.1% ± 3.4
OPCs 8.1% ± 3.4
SST neurons 0.1% ± 0.1
1.5% ± 0.5
2.2% ± 0.4
DLX6-AS1 neurons
26.6% ± 2.9
MSPNs
6.7% ± 2.9
Microglia
0.2% ± 0.2
Lymph
1% ± 0.5
Vasculature
9.2% ± 8.9
High-translation

Figure 1. Cellular composition of the adult human SEZ.
A) Experimental workflow. A.I) Dot plot depicting the age of the donors, per age group. Each dot indicates a sample and the horizontal line indicates the average age of the donors in the group. Young adults (Y-ad) and Middle-aged adults (M-ag). A.II) Fluorescence Activated Nucleus Sorting of $DAPI^+$ events for snRNAseq. **B)** UMAP depicting 36,626 nuclei from 8 donors. Colors indicate nuclei clusters resulting from unsupervised clustering analysis of nuclei transcriptomic profiles (dim = 30, k.parameter = 10, res = 0.4). **C)** Cluster marker genes. Top: dendrogram ordering the identified clusters based on hierarchical clustering results. Horizontal grey line indicates the cutoff level used to group clusters with similar transcriptomic profiles. Grouped clusters were annotated as same cell types. Bottom: Dot plot depicting a selection of representative marker genes of each cluster. Dot size indicates the fraction of nuclei expressing the gene and the color depicts the gene scaled average expression. **D)** Bar plot depicting the top enriched gene ontology term, for the more abundantly expressed genes, per cluster. Score: negative logarithm_{10} of the adjusted *p* value resulting from the enrichment analysis. **E)** Pie chart depicting the average proportion of each cell type, considering the 8 cases. Clusters were grouped based on the dendrogram depicted in C) and annotated based on the expression of cellular-specific marker genes and gene ontology enrichment analysis.

In summary, all major brain cell types were identified, including cell types with potential NSCs features.

The majority of adult human SEZ NSCs may be in a quiescent state

To further characterize the SEZ cell types expressing NSCs and/or neuronal genes, Astro/NSCs, ependymal cells, DLX6-AS1 neurons, SST neurons, MSPNs, and high-translation nuclei (Figure 2 A) were extracted from the dataset and subjected to enrichment and pseudotime analyses.

We did not find clusters enriched for proliferation- or cell cycle progression-related genes [8] (Figure 2 B). While a few nuclei expressed *PCNA*, a gene widely accepted as a proliferation marker, and therefore indicating some cells are proliferating; the *PCNA* expression did not seem to be a particular hallmark of any of the identified clusters expressing NSCs and/or neuronal marker genes. Thus, if neural progenitors and/or neural stem cells were present in these adult human SEZ samples, they were most likely in a quiescent state and not actively proliferating.

Because humans and mice share some neurogenic and neurodevelopmental features, including the postnatal neurogenic niches of the hippocampus and SEZ [68], some features of the SEZ cell types may also be conserved between human and mouse. We

evaluated the expression of adult mouse SEZ progenitor and neuronal marker genes in the subset of human NSCs/neuronal SEZ clusters. The mouse data was obtained from two single-cell transcriptomic studies [20, 21]. Consistent with the low expression of proliferation-related genes in the human SEZ (Figure 2 B), none of the human SEZ clusters were enriched for marker genes of mouse SEZ transient amplifiers (TAPs; Figure 2 C), or for marker genes of mouse “L clusters”, which were described as the most mitotically active mouse SEZ cell types [20, 21]. On the other hand, SST neurons (cluster 19), DLX6-AS1 (clusters 11, 13, and 14) and MSPNs (clusters 2, 3, 12, 10) neuronal clusters were enriched in the abundantly expressed genes by cluster N4 of Xie et al., 2020 [21], which was composed of mouse SEZ neurons (Figure 2 C). Moreover, our human MSPNs were enriched for genes highly expressed by the two MSPNs clusters found in mouse SEZ by Zywitza et al., 2018 [20]. These results corroborated the neuronal identity of clusters 19, 11, 13, 14, 2, 3, 12, and 10, and suggest that adult human and mouse SEZ neurons overlap in their highly expressed genes.

Although human Astro/NSCs clusters 16 and 0 were enriched in mouse niche astrocyte marker genes, they were also enriched in marker genes of clusters H1 and H2 of Xie, et al, which contained adult mouse quiescent neural stem cells (qNSCs; Figure 2 C). Astro/NSCs cluster 7 was also enriched in H2 qNSCs marker genes. The expression of marker genes of both mouse niche astrocytes and qNSCs in our Astro/NSCs clusters may indicate that astrocytes in the adult human SEZ maintain NSCs properties, as was previously suggested [69].

Interestingly, the high-translation cluster 9 was enriched in genes highly expressed by mouse neuroblasts and active neural stem cells (aNSCs), described by Zywitza, et al [20], indicating that even though these nuclei are not actively proliferating, they may be in a state that allows re-entry into the cell cycle. To identify the spatial distribution of this cell type in the human SEZ, we performed immunohistochemical (IMH) staining for JUND and PCSK1N, both genes abundantly expressed by the high-translation cluster (Figure 1D). JUND is a transcription factor that regulates cell proliferation [70-72], whereas PCSK1N is involved in neuropeptide processing [73]. JUND and PCSK1N positive cells showed a similar localization pattern in the human SEZ, with most labeled cells identified along the edge of the SEZ and occasional cells that appear to be moving away from the edge (Figure 2 D). Taken together, these observations

indicate that the high-translation cells are distributed as a layer adjacent to the ventricle.

Since the different cell types in the subset of nuclei expressing neuronal and/or NSCs marker genes may derived from each other during neurodevelopment or early post-natal years [1], we tested whether it was possible to detect and reconstruct a potential differentiation trajectory with adult transcriptomic data. We calculated a pseudotime trajectory based on the transition probability through the subset of nuclei expressing neuronal and/or NSCs marker genes, estimated with a random diffusion model (Figure 2 E.I) [29]. Instead of manually indicating the root cell type of the pseudotime, we used an automatized method that identifies the most distant nucleus, based on the diffusion model, from randomly selected nuclei in the dataset. The algorithm identified ependymal nuclei as the source of the pseudotime, which advanced towards the neuronal nuclei through the Astro/NSCs and high-translation nuclei (Figure 2 E.II). These observations further support a stem cell profile associated with Astro/NSCs and high-translation nuclei, and suggest that adult ependymal and NSCs in the ventricular sub-ventricular zone are sister cell types that derive from radial glial cells during neurodevelopment [52]. To identify the genes that potentially led the differentiation transitions, we used a recently published methodology that allows to identify the driver genes of non-linear pseudotime trajectories [30]. The most relevant genes, drivers of the pseudotime, are indicated in Figure 2 E.III. The expression of *CALM1* and *FRMPD4* increased along with the pseudotime, while *DPP10* expression increased from ependymal nuclei to Astro/NSCs and then decreased towards neuronal nuclei. Also, *HSPA1A* expression increased from ependymal to Astro/NSCs, reaching the highest expression activity in high-translation nuclei and then decreasing towards neurons. Conversely, the expression activity of *KCNIP4*, *ROBO2*, *DCC*, and *MCTP1* varied locally within the subset of neuronal nuclei; therefore, these genes may constitute drivers of neuronal maturation. The driver genes of the pseudotime (Figure 2 E.III) may constitute important modulators of the cellular differentiations that occurred in this brain region, possibly during earlier life stages.

Next, we tested whether the human SEZ clusters expressing neuronal or NSCs marker genes were enriched for genes associated with neurodevelopmental disorders that also have reported alterations in the SEZ, such as schizophrenia [5, 74], bipolar disorder [5], and autism [17, 75]. This may identify cell types affected by the underlying

genetics of the neurodevelopmental disorders. Several neuronal clusters were enriched for genes associated with schizophrenia (Figure 2 F), including SST neurons, DLX6-AS1 neurons that also abundantly expressed *RELN* (cluster 14, Figure 1 C) and two clusters of MSPNs (clusters 3 and 12). A previous study using single-cell transcriptomic data from different regions of the mouse brain, also indicated that schizophrenia associated genes are expressed in interneurons and MSPNs, but not in progenitor or glia cells [31]. We did not detect genes associated with bipolar disorder or autism enriched for any SEZ neuronal or NSCs clusters, indicating that SEZ cell types may not be genetically affected in autism or bipolar disorder.

In summary, our data show the majority of potential NSCs in the adult human SEZ are quiescent. However, the high-translation cluster appears to contain nuclei in a state that is more likely to re-enter the cell cycle, as compared to other SEZ clusters. Pseudotime analysis revealed a possible neurodevelopmental differentiation trajectory, and we show this data set can be used to further explore which SEZ cell types are potentially affected by the genetics of different neurodevelopmental diseases.

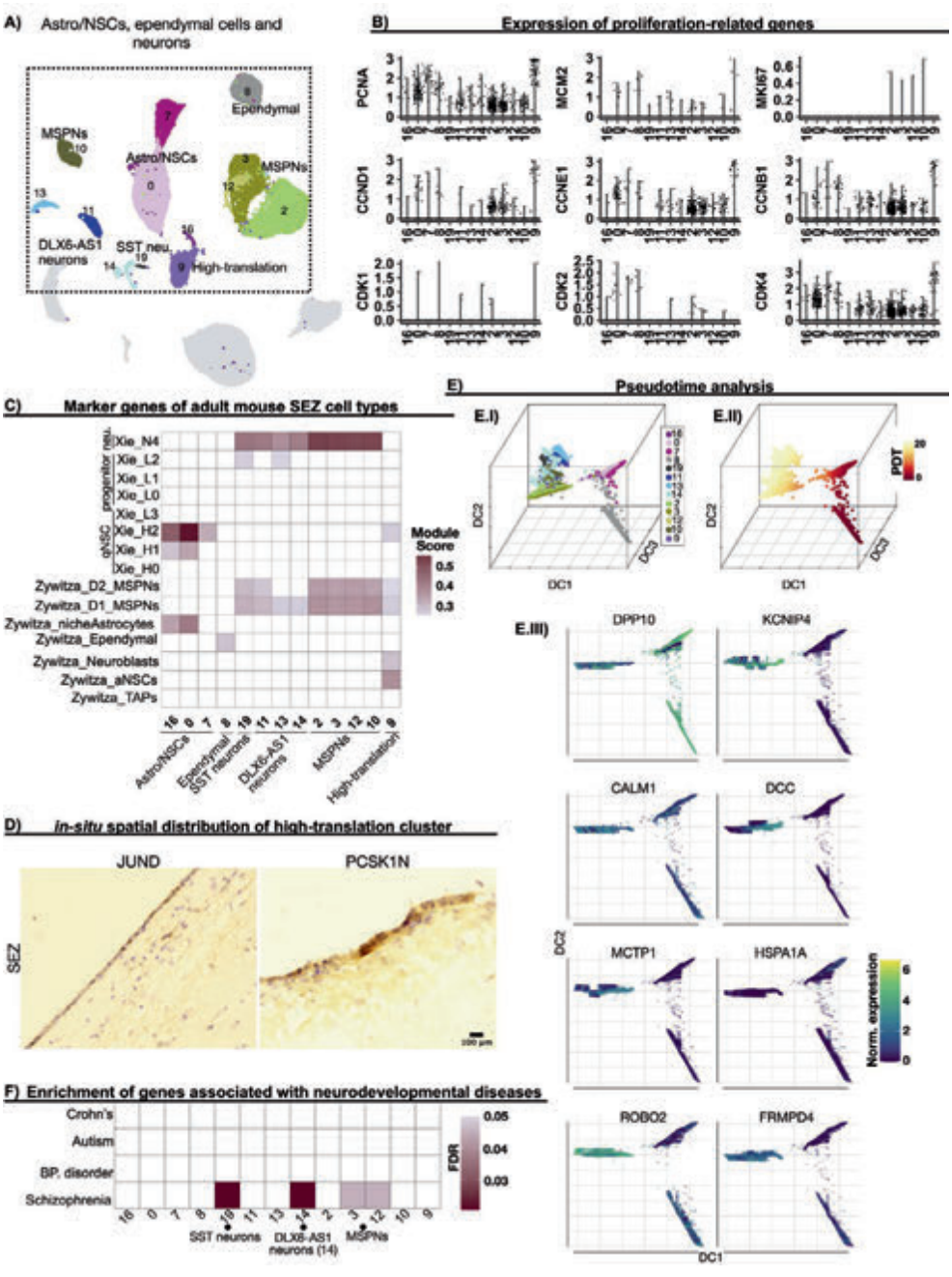
A) Astro/NSCs, ependymal cells and neurons
Ependymal
MSPNs
Astro/NSCs
MSPNs
DLX6-AS1 neurons
SST neu.
High-translation
B) Expression of proliferation-related genes
PCNA
MCM2
MKI67
CCND1
CCNE1
CCNB1
CDK1
CDK2
CDK4
C) Marker genes of adult mouse SEZ cell types
Xie_N4
Xie_L2
Xie_L1
Xie_L0
Xie_L3
Xie_H2
Xie_H1
Xie_H0
Zywitza_D2_MSPNs
Zywitza_D1_MSPNs
Zywitza_nicheAstrocytes
Zywitza_Ependymal
Zywitza_Neuroblasts
Zywitza_aNSCs
Zywitza_TAPs
Module Score
Astro/NSCs
Ependymal SST neurons
DLX6-AS1 neurons
MSPNs
High-translation
D) in-situ spatial distribution of high-translation cluster
JUND
PCSK1N
SEZ
E) Pseudotime analysis
E.I)
E.II)
PDT
DC1
DC2
DC3
E.III)
DPP10
KCNIP4
CALM1
DCC
MCTP1
HSPA1A
ROBO2
FRMPD4
Norm. expression
F) Enrichment of genes associated with neurodevelopmental diseases
Crohn's
Autism
BP. disorder
Schizophrenia
FDR
SST neurons
DLX6-AS1 neurons (1-4)
MSPNs

Figure 2. Profiling of SEZ clusters expressing NSCs and neuronal marker genes.

A) UMAP highlighting Astro/NSCs, high-translation, ependymal and neuronal nuclei, which were extracted and further characterized. **B)** Violin plots depicting the expression level of a set of genes associated with proliferation, in each cluster. The clusters do not have particularly high expression of these genes. **C)** Heatmap depicting average module scores of gene sets associated with mouse SEZ cell types (Xie, et al., 2020 and Zywitza, et al., 2018). **D)** Representative IMH of JUND and PCSK1N in paraffin embedded and fresh adult human SEZ sections, respectively. **E)** Pseudotime analysis. E.I) Nuclei are ordered in a three-dimensional diffusion map. Colors indicate original nuclei clusters. E.II) Pseudotime (PDT) estimation, indicated in a color code, calculated based on the diffusion components. The root cell (origin of the pseudotime trajectory) was automatically identified. The pseudotime trajectory reveals a progression from the ependymal to the neuronal nuclei, going through the Astro/NSCs and high-translation nuclei. E.III) Two-dimensional differential maps of the most relevant genes driving the pseudotime depicted in E.II. Arrows indicate the nuclei estimated change in gene expression activity, calculated from partial derivatives with respect to the embedding. Color of the arrow indicates gene expression level in each nucleus. **F)** Heatmap depicting the association of gene sets related to different neurodevelopmental diseases with our Astro/NSCs, high-translation, ependymal and neuronal clusters. Color code indicates the FDR corrected *p* value obtained from associating the particular gene set with each cluster. Crohns' related gene set was used as a negative control.

The transcriptomic profile of neuronal and non-neuronal cell types changes between early and middle adulthood

Having identified the cellular identity of all the different SEZ clusters, we then tested for potential differences in the transcriptomic profiles between the two age groups. First, we aggregated the count data derived from each sample and performed a principal component analysis (PCA; Figure 3 A). Almost all the samples, except sample F, segregated in the PCA plot based on their age, indicating age-associated differences in the SEZ transcriptomes. We compared the transcriptomic profiles between M-ag and Y-ad samples for each SEZ cluster to identify the cell types contributing to the transcriptional differences between the two age groups. With an absolute $\log_2$FC > 0.25 and adjusted *p* value < 0.05, we identified 569 differentially expressed genes (DEGs; Figure 3 B, S. Figures 1 and 2, and S. Table 4). Across different cell types, some genes, such as *ANO4*, *PBX3*, *MAN2A1*, *FLRT2*, *GABRA2*, *CPE*, *RAB3C*, *SEMA6D*, *ADGRL3*, *CNTN4*, and *HS3ST5*, were expressed lower in M-ag than in Y-ad, while *SLC6A1-AS1*, *EPB41L2*, and *ITPKB* were expressed higher in

M-ag than Y-ad (S. Table 5), suggesting a generalized effect of age on the expression of these genes that affects different cell types.

Both non-neuronal (S. Figure 1) and neuronal clusters (S. Figure 2) exhibited DEGs between M-ag and Y-ad. Ependymal cells had the highest number of DEGs between the two age groups (Figure 3 B; 176 DEGs). Gene ontology enrichment analysis indicated that genes highly expressed in Y-ad ependymal cells, including *SHROOM3*, *SOX9*, *EFNA5*, *S100A10*, *FGFR2*, *VIM*, among many others, were enriched for “actin filament-based process”, “cytoskeleton organization” and “nervous system development” (Figure 3 C). The highly expressed genes in Y-ad Astro/NSCs cluster 7, including *CECR2*, *CDH4*, *PTPRM, SEMA6D*, and *SEMA5A*, were also enriched for the gene ontology term “nervous system development”.

Oligodendrocytes of cluster 5 exhibited the second highest number of DEGs between M-ag and Y-ad. The highly expressed genes in Y-ad oligodendrocytes of cluster 5, such as *HECW2*, *DISC1*, *FUT9*, *TNIK*, and *MACF*, were enriched in “regulation of cellular process” and “generation of neurons” (Figure 3 C). In contrast, the highly expressed genes in M-ag oligodendrocytes, such as *B2M*, *ITPKB*, *SH3RF1*, and *CD81*, were related to “regulation of alpha-beta T cell activation” (Figure 3 D).

For neuronal clusters (S. Figure 2), the MSPNs nuclei of clusters 2 and 10 exhibited higher expression of genes such as *RELN*, *SYT4*, *CNTN4*, *FLRT2*, and *NPAS2*, related to “nervous system development” (Figure 3C), in Y-ad as compared to M-ag. Likewise, the genes highly expressed in Y-ad MSPNs of cluster 3, such as *NREP*, *PTPRD*, *SLIT2*, *IL1RAPL1*, and *HDAC9*, were related to “generation of neurons”. In contrast, M-ag DLX6-AS1 neuronal cluster 11 exhibited higher expression of genes such as *DHX36*, *EIF4A2*, and other genes coding for ribosomal proteins (*RP*), related to “cytoplasmic translation”, “cellular macromolecule biosynthetic process”, and “ribosome biogenesis”. The highly expressed genes in M-ag MSPNs of cluster 2 were also related to “cytoplasmic translation”, and included genes coding for different *RP* genes (Figure 3 D).

These results indicate that, age affects the transcriptomic profile of non-neuronal as well as neuronal nuclei. The expression of genes related to nervous system development was higher in early as compared to middle adulthood, suggesting the potential for central nervous system (CNS) development during early adulthood that may

decline in middle age. In contrast, genes related to translation and to immune activation were highly expressed in middle adulthood, in neuronal and oligodendrocyte clusters, respectively. Additionally, the expression of some genes was affected by age across different clusters, which may constitute a transcriptional hallmark of age that involves different cell types.

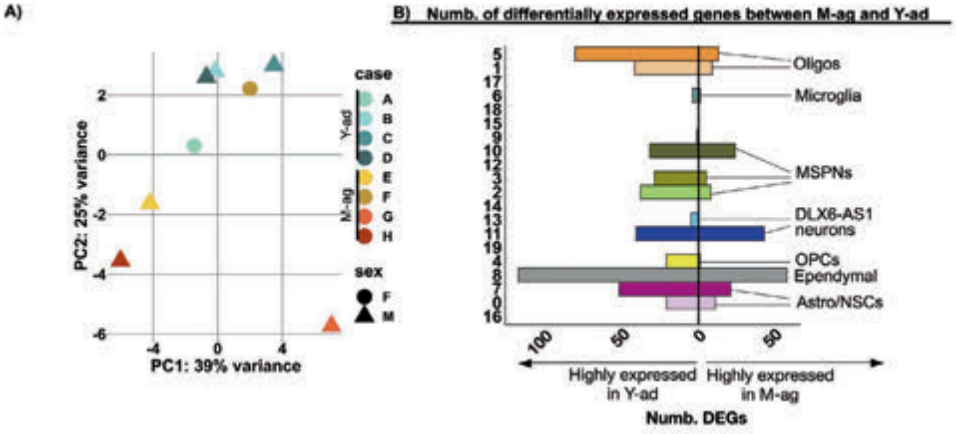
A)
B) Numb. of differentially expressed genes between M-ag and Y-ad
PC2: 25% variance
PC1: 39% variance
case
Y-ad
M-ag
A
B
C
D
E
F
G
H
sex
F
M
Oligos
Microglia
MSPNs
DLX6-AS1 neurons
OPCs
Ependymal
Astro/NSCs
Highly expressed in Y-ad
Highly expressed in M-ag
Numb. DEGs

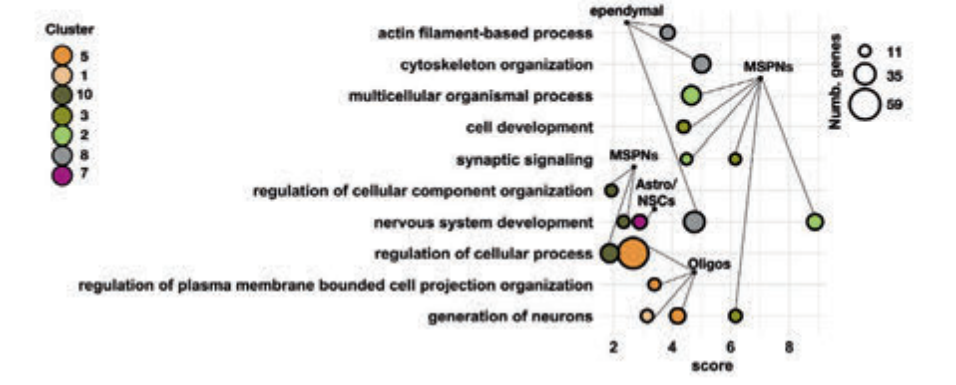
C) Gene ontology enrichment analysis of highly expressed genes in Y-ad
Cluster
5
1
10
3
2
8
7
ependymal
actin filament-based process
cytoskeleton organization
multicellular organismal process
cell development
synaptic signaling
regulation of cellular component organization
nervous system development
regulation of cellular process
regulation of plasma membrane bounded cell projection organization
generation of neurons
MSPNs
Astro/ NSCs
Oligos
Numb. genes
11
35
59
score

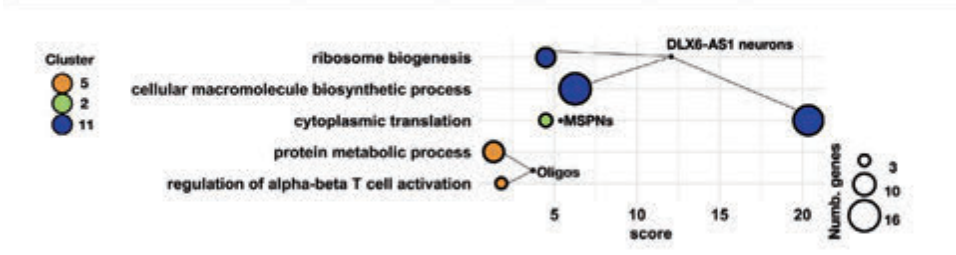
D) Gene ontology enrichment analysis of highly expressed genes in M-ag
Cluster
5
2
11
ribosome biogenesis
cellular macromolecule biosynthetic process
cytoplasmic translation
protein metabolic process
regulation of alpha-beta T cell activation
DLX6-AS1 neurons
MSPNs
Oligos
Numb. genes
3
10
16
score

Figure 3. Differences in the transcriptomic profiles of SEZ cell types between middle-aged and young adults.
A) Principal component analysis of pseudobulked samples. Count data derived from the same sample were aggregated and principal component analysis was performed. Each point indicates a case, and its shape reflects the sex of the donor. Young adults (Y-ad) and Middle-aged adults (M-ag). **B)** Bar plot depicting the number of identified differentially expressed genes (DEGs) between M-ag and Y-ad (absolute log_2FC > 0.25 and FDR adjusted *p* value < 0.05, detailed in Methods), across the different clusters. **C)** Scatter plot depicting the top three significantly enriched terms in the highly expressed genes in Y-ad, across the different clusters. The color of the dot indicates the cluster, and its size indicates the number of intersected genes between the list of DEGs and the genes associated with the particular term. Lines/edges connect clusters corresponding to the same cell type, defined with hierarchical clustering analysis in Figure 1 E. Score: negative $logarithm_{10}$ of the adjusted *p* value resulting from the enrichment analysis. **D)** Scatter plot depicting the top three significantly enriched terms in the highly expressed genes in M-ag, across the different clusters.

The relative abundance of OPCs in the adult SEZ declines along with age

To determine if the cellular composition of the SEZ was affected by age, we used generalized linear modelling to compare the proportion of each SEZ cluster between M-ag and Y-ad. We did not detect differences in the relative abundance of any Astro/NSCs cluster, nor in the relative abundance of the high-translation cluster, between the two age groups, suggesting that the pool of potential NSCs remained stable during the investigated age range (S. Figure 3).

The proportion of OPCs and microglia was reduced in M-ag as compared to Y-ad (Figure 4 A.I and A.II). In contrast, the proportion of the neuronal cluster DLX6-AS1 13 was increased in M-ag (Figure 4 A.III). Among the neuronal clusters expressing *DLX6-AS1* (Figure 4 A.IV), cluster 13 had the highest *SFRP1* expression activity. SFRP1 is a Wnt antagonist that inhibits cell proliferation [8].

To determine if these observations could be replicated in another dataset using a different methodology, we used bulk RNA sequencing data from human SEZ samples of donors of 4 different age groups (Figure 4 B) to estimate the proportions of human SEZ clusters, identified with snRNAseq. We observed a significant decrease in the relative abundance of OPCs in aged adults (average age=86) with respect to young adults (average age=23) and adolescents (average age=16.5). This corroborates the decline in OPCs associated with age that we detected in our snRNAseq data. In

contrast, the differences in the relative abundance of microglia and DLX6-AS1 cluster 13 associated with age were not observed in the bulk RNAseq profiles.

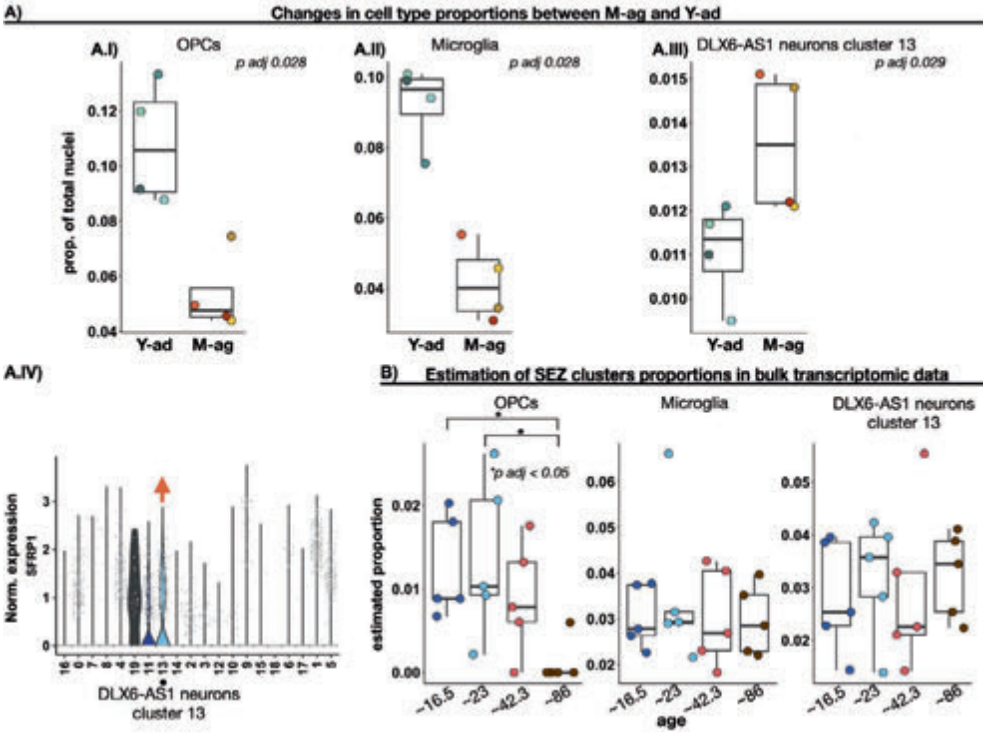

Figure 4. The relative abundance of SEZ OPCs, microglia and DLX6-AS1 neurons of cluster 13 differed between middle-aged and young adults.

A) SEZ cell types with different relative abundance between M-ag and Y-ad. A.I) Box plots depicting the proportion of OPCs, microglia and DLX6-AS1 neurons (cluster 13) in Y-ad and M-ag. Each dot indicates a sample and horizontal lines indicate the median. Group comparison (Y-ad vs M-ag) was carried out with a generalized linear model and *p* values were Bonferroni corrected. A.II) Violin plots depicting *SFRP1* expression level in each cluster. DLX6-AS1 neurons of cluster 13, which are more abundant in M-ag, highly express *SFRP1*. **B)** Box plots depicting the estimated proportion of OPCs, microglia and DLX6-AS1 neurons cluster 13 in 4 different age groups. Proportions were estimated by deconvoluting bulk RNA sequencing data of the SEZ from 20 donors on the transcriptomic profiles of the SEZ clusters identified in snRNAseq. The average age of the donors in each group is indicated in the x axis. Group comparison for the relative abundance of OPCs, microglia and DLX6-AS1 neurons cluster 13 was performed with Kruskal Wallis test, and a Dunn post hoc analysis was performed for OPCs. *p* values resulting from the Dunn Test were FDR corrected. * indicates adj. *p* value <0.05.

Taken together, these results indicate a significant decrease in the proportion of OPCs in middle aged SEZs. The change in the relative abundance of microglia and DLX6-AS1 neurons of cluster 13 that we detected in the M-ag SEZ may be too subtle or inconsistent to be detected in bulk RNA sequencing data.

Discussion

We analyzed the cells in the human SEZ of young and middle-aged adults (Y-ad, M-ag) with snRNAseq and while several clusters expressed NSCs marker genes, no cluster was enriched for proliferation-related genes, indicating that NSCs in the adult SEZ are likely in a dormant state. The expression of genes related to nervous system development was reduced in M-ag as compared to Y-ad, indicating that CNS development may continue in early adulthood but decline in middle age. Furthermore, we found the relative abundance of OPCs declines in middle age and the cellular composition of the human SEZ is remodeled during the age range investigated.

The co-expression of niche astrocyte and NSCs marker genes in the Astro/NSCs clusters is consistent with other studies suggesting astrocytes are the NSCs in the adult human SEZ [69]. In addition, the low expression of proliferation-related genes in the NSCs of the adult SEZ is consistent with other studies proposing neurogenesis as a rare event in the adult human brain [16, 76-78]. Interestingly, the high-translation nuclei (cluster 9) were enriched in genes highly expressed by both mouse neuroblasts and active NSCs (aNSCs) [20]. Single-cell transcriptomic studies of the mouse brain found increased expression of transcription and translation related genes in aNSCs [20, 21, 24], suggesting that translational activation is one of the earliest events on the way out of quiescence [24]. Thus, the high-translation nuclei of cluster 9 may be in a “primed” state that under certain conditions, such as brain injury, could re-enter the cell cycle [24]. In the adult mouse brain, the transition from dormant NSCs to neuronal progenitors does not involve changes in cell identity, but rather reflects a conversion between a quiescent and an activated state [79]. Our pseudotime analysis identified *HSPA1A* expression as the driver of the transition between Astro/NSCs and the high-translation cluster, reaching an expression peak in high-translation nuclei and decreasing towards neurons. *HSPA1A* codes for a 70kDa heat shock protein (Hsp70), and high *HSPA1A* expression activity has been associated with increased proliferation in cancer cells [80], including glioma [81]. The expression level of *HSPA1A* may also modulate the cell cycle under physiological conditions and, therefore, participate in the

regulation of the possible transition between inactive and active NSCs states. Future experiments tuning *HSPA1A* expression activity in mouse or human derived NSCs could help to identify the possible role of *HSPA1A* in the regulation of NSCs dormancy.

In humans, the number of progenitor cells in the SEZ decreases during first postnatal year, drastically reducing the neurogenic potential in this region [2, 82, 83]. In contrast, we did not identify changes in the relative abundance of NSCs (Astro/NSCs or high-translation cluster) between the two age groups, suggesting that the pool of SEZ NSCs does not decline between early and middle adulthood. However, the lower expression of genes related to nervous system development in Astro/NSCs, ependymal and neuronal nuclei of M-ag might reflect a reduced neurogenic potential of the SEZ in middle adulthood. Indeed, the SEZ qNSCs from older mice are more resistant to injury-induced activation than NSCs from young mice [84]. In addition, we identified higher expression of genes related to immune activation in oligodendrocytes of M-ag. Bulk transcriptomic data also indicated immune activation associated with aging in the human SEZ [18]. Inflammatory signals derived from this cellular niche promote quiescence of NSCs in the mouse SEZ [84, 85]. Our results suggest that oligodendrocytes are contributing to the increase in pro-inflammatory signals associated with age in the human SEZ, and could decrease the probability of qNSCs to reenter the cell cycle during middle adulthood.

The expression levels of particular genes differed between M-ag and Y-ad across different cell types, and may indicate a transcriptional hallmark of age that affects several cell types. For instance, MSPNs, Astro/NSCs, and ependymal cells all depicted lower *CPE* expression activity in M-ag. Lower CPE expression is associated with learning and memory decline in mouse [86, 87], and even though there is variability among adults, some cognitive abilities decline with age [88], and low *CPE* expression in middle adulthood might contribute to this. In addition, the expression of *MAN2A1* was lower in DLX6-AS1 and MSPNs of M-ag. A previous study reported a positive association between *MAN2A1* expression and global cognitive scores [89]; therefore, low *MAN2A1* expression in M-ag donors may also be related to cognitive impairment associated with age. Conversely, *SLC6A1-AS1* expression was enriched in the DLX6-AS1 and MSPNs cell types of M-ag. High *SLC6A1-AS1* expression was associated with overall survival from cholangiocarcinoma [90], suggesting a potential inhibitory effect of SLC6A1-AS1 on cellular proliferation. Thus, the high expression of *SLC6A1-*

AS1 in M-ag DLX6-AS1 and MSPNs might be related to a reduced proliferative potential during middle adulthood.

On the other hand, some changes in gene expression between early and middle adulthood may reflect protective mechanisms to age-related brain damage, such as axonal degeneration [91]. For instance, the expression of *SEMA6D*, an axon guidance molecule [92], was lower in OPCs, Astro/NSCs, and MSPNs of M-ag as compared to Y-ad. SEMA6D expression is increased in the surrounding cells of injured axons, acting as an axon repellent that impairs axonal regrowth [92]. Therefore, the reduced expression of *SEMA6D* in M-ag might reflect a buffering mechanism for axonal degeneration that occurs during normal aging.

While we only identify a few DEGs between M-ag and Y-ad OPCs, we detected a decrease in OPCs relative abundance associated with age. There is an age-related reduction in the re-myelination potential of the CNS. This is reflected in normal aging by reductions in white matter volume across different brain regions [93], associated with a decline in cognitive performance, and hallmarks of white matter degradation [94]. Age-related impairment of CNS re-myelination capacity is also manifested in pathological conditions. For instance, patients with multiple sclerosis frequently transit from a relapsing-remitting to a progressive form of the disease around the age of 45 ± , with irreversible worsening of lesions and neurologic function [95]. Interestingly, *post-mortem* analysis of SEZ tissue from patients with multiple sclerosis indicated increased number of proliferating OPCs, suggesting that SEZ contributes OPCs that are available to migrate to periventricular lesions, to promote re-myelination of CNS [96]. Thus, the lower proportion of SEZ OPCs in middle adulthood may constitute an age-related feature that contributes to the age-related decline in CNS re-myelination efficiency.

The relative abundance of microglia was decreased in M-ag as compared to Y-ad. A decline in the proportion of SEZ microglia between early and middle adulthood may constitute a hallmark of age particular to this brain region, and could precede the altered microglia phenotypes identified in the brain at later stages of life, during aging [97-99]. Conversely, the proportion of DLX6-AS1 neuronal cluster 13, which highly expressed *DLX6-AS1* and *EGFR*, together with *SFRP1*, was greater in M-ag donors. Donega, et al., 2022 [8], demonstrated an increase in the number of SFRP1 positive cells in the human SEZ associated with aging, and proposed SFRP1 as a target for reactivating neuronal progenitor cells. Thus, if the SEZ neuronal clusters highly expressing *DLX6-AS1*

(clusters 11, 13 and 14) correspond to immature neurons, the higher relative abundance of DLX6-AS1 neurons expressing *SFRP1* (cluster 13) in M-ag could be reflecting a reduction in the proliferative potential of SEZ immature neurons in middle adulthood. However, the difference between M-ag and Y-ad in microglia and cluster 13 proportions was not identified in the bulk RNAseq profiles, suggesting that these results might be inconsistent and further investigation with larger sample sizes is required to validate them.

Some limitations may be considered when interpreting the results presented in this study. First, we were not able to discriminate between astrocytes and NSCs. As mentioned above, it may be that astrocytes constitute the NSCs in the adult human SEZ [69]. However, the lack of knowledge regarding specific marker genes for these cell types [100] could also explain our inability to discriminate against them. Also, because of the few nuclei expressing *Ki67* and/or *PCNA* (~5 ki67 positive cells/50um of SEZ section [78]), we may be underpowered to detect proliferating NSCs as a separate cluster of nuclei with snRNAseq. This may preclude the identification of a NSC cluster in active cycle, limiting our ability to delve into potential differences in NSCs proliferation rate between early and middle adulthood.

In summary, the NSCs of the adult human SEZ seem to be primarily in a quiescent state and their relative abundance is stable between early and middle adulthood. Nevertheless, age affects the transcriptomic profile of several adult SEZ cell types, particularly reducing the expression of genes related to nervous system development. In addition, the relative abundance of OPCs decreases with age in the human SEZ, probably debilitating the re-myelination efficiency of the CNS. Our results identify the cell types and genes particularly affected by age in the human SEZ, and may identify key targets for influencing the neurogenic capacity of this niche and for the development of preventive treatments for age-related brain changes.

Acknowledgments

The authors would like to thank Nieske Brouwer and Emma Gerrits for their support during the nuclei isolation procedure. The authors would like to thank Geert Mesander, Johan Teunis and Theo Bijma from the UMCG flow cytometry unit for sorting of the nuclei. We thank Pravina Patel for immunohistochemistry.

Financial support and sponsorship

This study was supported by The Stanley Medical Research Institute.

S.P is a recipient of “Agencia Nacional de Investigación y Desarrollo de Chile” (#21181102) and “Graduated School of Medical Sciences, University of Groningen” fellowships for PhD studies.

Conflicts of interest

The authors declare no conflict of interest.

Availability of supporting data

All the data are available through the SMRI website, www.stanleyresearch.org or directly at www.sncid.stanleyreserach.org.

Supplementary information is available at MP’s website.

Author contributions

M.W, C.S and B.J.L.E conceived and supervised the study. M.W characterized the cohort and provided the samples. S.P and A.A performed the experiments. S.P analyzed and visualized the data, and wrote the first draft of the manuscript. All authors contributed to project design, interpretation of the results and writing of the manuscript.

Supplemental information

Supplementary Figure 1. Differentially expressed genes between middle-aged and young adults in non-neuronal clusters.
Heatmaps depicting scaled expression level of the differentially expressed genes between Y-and M-ag (absolute $log_2FC > 0.25$ and FDR adjusted *p* value < 0.05, detailed in Methods) in **A)** Oligodendrocytes cluster 1, **B)** Oligodendrocytes cluster 5, **C)** Ependymal cells cluster 8 and **D)** Astro/NSCs cluster 7.

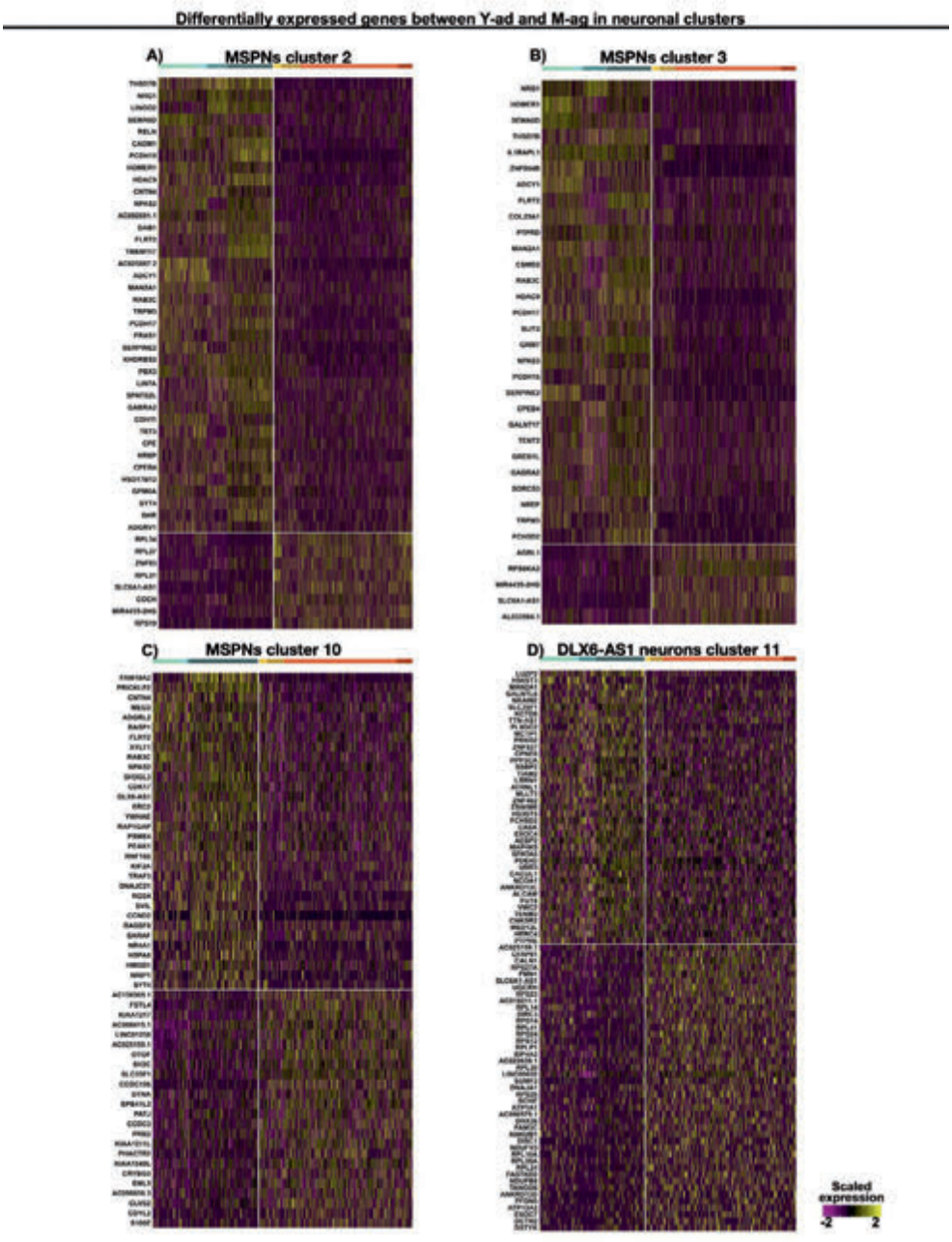
Differentially expressed genes between Y-ad and M-ag in neuronal clusters
A)
MSPNs cluster 2
B)
MSPNs cluster 3
C)
MSPNs cluster 10
D)
DLX6-AS1 neurons cluster 11
Scaled expression
-2
2

Supplementary Figure 2. Differentially expressed genes between middle-aged and young adults in neuronal clusters.
Heatmaps depicting scaled expression level of the differentially expressed genes between Y-and M-ag (absolute $log_2FC > 0.25$ and FDR adjusted *p* value < 0.05, detailed in Methods) in **A)** MSPNS cluster 2, **B)** MSPNs cluster 3, **C)** MSPNs cluster 10 and **D)** DLX6-AS1 neurons cluster 11.

Proportions of all clusters in M-ag and Y-ad

A)

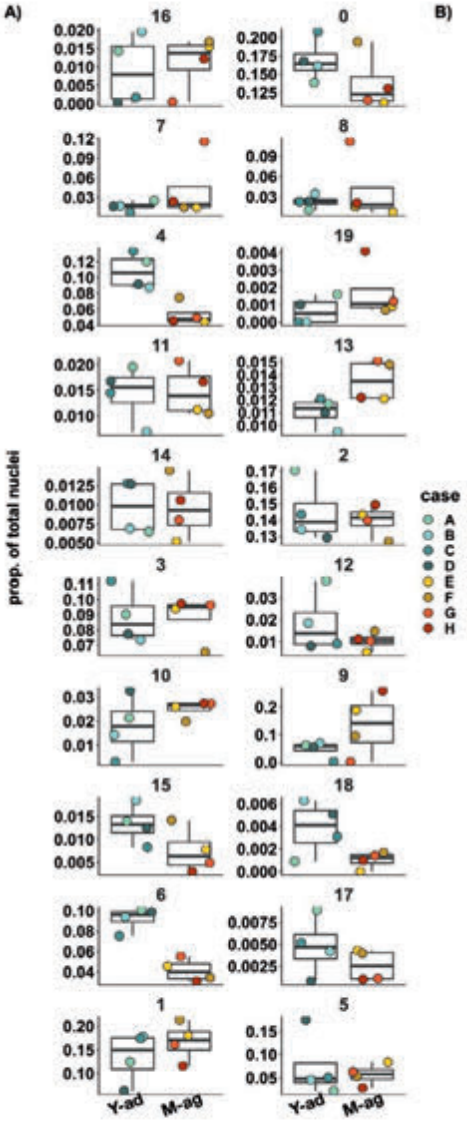

B)

cluster	cell type	M-ag coef	*p* value	adj *p* value
16	Astro/NSCs	-0.28	0.80	0.84
0	Astro/NSCs	-0.31	0.12	0.30
7	Astro/NSCs	1.67	0.04	0.16
8	Ependymal	1.44	0.05	0.16
4	OPCs	-0.76	0.00	0.03
19	SST neurons	0.47	0.45	0.69
11	DLX6-AS1 neurons	0.14	0.49	0.70
13	DLX6-AS1 neurons	0.27	0.00	0.03
14	DLX6-AS1 neurons	-0.14	0.56	0.72
2	MSPNs	-0.03	0.69	0.77
3	MSPNs	0.07	0.61	0.72
12	MSPNs	-0.48	0.35	0.59
10	MSPNs	0.16	0.58	0.72
9	High-translation	0.04	0.97	0.97
15	Vasculature	-0.74	0.06	0.18
18	Lymphocytes	-1.05	0.04	0.16
6	Microglia	-0.70	0.00	0.03
17	Oligodendrocytes	-0.87	0.24	0.48
1	Oligodendrocytes	0.45	0.15	0.34
5	Oligodendrocytes	-0.55	0.32	0.58

Supplementary Figure 3. Proportions of SEZ clusters in middle-aged and young adults.
A) Boxplots depicting the proportion of all SEZ clusters in Y-ad and M-ag. Each dot indicates a sample and horizontal lines indicate the median. **B)** Table depicting the results from comparing the relative abundance of each cluster between Y-ad and M-ag. Group comparison was carried out with generalized linear modeling and *p* values were Bonferroni corrected. M-ag coef is the value estimated for the coefficient associated with the M-ag variable in the regression model (effect of the M-ag group on the probability that a nucleus belongs to a particular cluster).

Supplementary Table 1. Information about the cases used in this study.

case	age	group	sex	ethnicity	PMI	RIN	% transcripts mapped to the genome	# seq. nuclei
A	16.5	Y-ad	F	White	16	8.5	82.1	4,275
B	18	Y-ad	M	White	40	8.5	75.3	1,892
C	21.9	Y-ad	M	Black	7	7.4	66.9	2,888
D	22	Y-ad	M	White	24	8.1	60.6	7,259
E	46	M-ag	M	Black	18	8.8	77.7	1,159
F	48	M-ag	F	White	12	7	76.9	2,966
G	53	M-ag	M	White	34	8.4	69.6	14,213
H	53	M-ag	M	White	28	7.3	78.3	1,974

Information about the cases and quality measurements of the SEZ samples obtained from them. Post Mortem Interval (PMI), Sequencing (Seq), Young adults (Y-ad), Middle-aged adults (M-ag).

Supplementary Table 2. Comparison of demographics between the age groups.

variables	normal	hom_var test	hom_var	comparison test	*p* value	consider
age	FALSE	Levene	TRUE	Wilcox	0.029	TRUE
PMI	TRUE	F-test	TRUE	t-test	0.889	FALSE
pct_mapped	TRUE	F-test	TRUE	t-test	0.424	FALSE
RIN	TRUE	F-test	TRUE	t-test	0.637	FALSE

Results of comparing case-related variables between Y-ad and M-ag. Homoscedasticity of the variance (Hom_var), Percentage mapped to the genome (pct_mapped).

Supplementary Table 3. Highly expressed genes per cluster.

Supplementary Table 4. Differentially expressed genes in M-ag as compared to Y-ad in each cluster.

Supplementary Table 5. Genes with different expression level between M-ag and Y-ad across multiple cell types.

References

1. Doetsch, F. and A. Alvarez-Buylla, *Network of tangential pathways for neuronal migration in adult mammalian brain.* Proceedings of the National Academy of Sciences, 1996. **93**(25): p. 14895-14900.
2. Sanai, N., T. Nguyen, R.A. Ihrie*, et al.*, *Corridors of migrating neurons in the human brain and their decline during infancy.* Nature, 2011. **478**(7369): p. 382-386.
3. Cipriani, S., I. Ferrer, E. Aronica*, et al.*, *Hippocampal Radial Glial Subtypes and Their Neurogenic Potential in Human Fetuses and Healthy and Alzheimer's Disease Adults.* Cereb Cortex, 2018. **28**(7): p. 2458-2478.
4. Weissleder, C., M.A. Kondo, C. Yang*, et al.*, *Early-life decline in neurogenesis markers and age-related changes of TrkB splice variant expression in the human subependymal zone.* Eur J Neurosci, 2017. **46**(2): p. 1768-1778.
5. Weissleder, C., H.F. North, M. Bitar*, et al.*, *Reduced adult neurogenesis is associated with increased macrophages in the subependymal zone in schizophrenia.* Mol Psychiatry, 2021. **26**(11): p. 6880-6895.
6. Eriksson, P.S., E. Perfilieva, T. Björk-Eriksson*, et al.*, *Neurogenesis in the adult human hippocampus.* Nature Medicine, 1998. **4**(11): p. 1313-1317.
7. Dennis, C.V., L.S. Suh, M.L. Rodriguez*, et al.*, *Human adult neurogenesis across the ages: An immunohistochemical study.* Neuropathol Appl Neurobiol, 2016. **42**(7): p. 621-638.
8. Donega, V., A.T. van der Geest, J.A. Sluijs*, et al.*, *Single-cell profiling of human subventricular zone progenitors identifies SFRP1 as a target to re-activate progenitors.* Nature Communications, 2022. **13**(1): p. 1036.
9. Curtis Maurice, A., B. Penney Ellen, G. Pearson Andree*, et al.*, *Increased cell proliferation and neurogenesis in the adult human Huntington's disease brain.* Proceedings of the National Academy of Sciences, 2003. **100**(15): p. 9023-9027.
10. Leonard, B.W., D. Mastroeni, A. Grover*, et al.*, *Subventricular zone neural progenitors from rapid brain autopsies of elderly subjects with and without neurodegenerative disease.* J Comp Neurol, 2009. **515**(3): p. 269-94.
11. van den Berge, S.A., M.E. van Strien, J.A. Korecka*, et al.*, *The proliferative capacity of the subventricular zone is maintained in the parkinsonian brain.* Brain, 2011. **134**(11): p. 3249-3263.
12. Gault, N. and F.G. Szele, *Immunohistochemical evidence for adult human neurogenesis in health and disease.* WIREs Mechanisms of Disease, 2021. **13**(6): p. e1526.
13. Shen, Q., K. Goderie Susan, L. Jin*, et al.*, *Endothelial Cells Stimulate Self-Renewal and Expand Neurogenesis of Neural Stem Cells.* Science, 2004. **304**(5675): p. 1338-1340.
14. Környei, Z., E. Gócza, R. Rühl*, et al.*, *Astroglia-derived retinoic acid is a key factor in glia-induced neurogenesis.* Faseb j, 2007. **21**(10): p. 2496-509.
15. Vedam-Mai, V., B. Gardner, M.S. Okun*, et al.*, *Increased precursor cell proliferation after deep brain stimulation for Parkinson's disease: a human study.* PLoS One, 2014. **9**(3): p. e88770.
16. Macas, J., C. Nern, K.H. Plate*, et al.*, *Increased generation of neuronal progenitors after ischemic injury in the aged adult human forebrain.* J Neurosci, 2006. **26**(50): p. 13114-9.
17. Kotagiri, P., S.A. Chance, F.G. Szele*, et al.*, *Subventricular zone cytoarchitecture changes in autism.* Dev Neurobiol, 2014. **74**(1): p. 25-41.
18. Bitar, M., C. Weissleder, H.F. North*, et al.*, *Identifying gene expression profiles associated with neurogenesis and inflammation in the human subependymal zone from development through aging.* Scientific Reports, 2022. **12**(1): p. 40.
19. Tang, F., C. Barbacioru, Y. Wang*, et al.*, *mRNA-Seq whole-transcriptome analysis of a single cell.* Nature Methods, 2009. **6**(5): p. 377-382.
20. Zywitza, V., A. Misios, L. Bunatyan*, et al.*, *Single-Cell Transcriptomics Characterizes Cell Types in the Subventricular Zone and Uncovers Molecular Defects Impairing Adult Neurogenesis.* Cell Reports, 2018. **25**(9): p. 2457-2469.e8.
21. Xie Xuanhua, P., R. Laks Dan, D. Sun*, et al.*, *High-resolution mouse subventricular zone stem-cell niche transcriptome reveals features of lineage, anatomy, and aging.* Proceedings of the National Academy of Sciences, 2020. **117**(49): p. 31448-31458.

22. Mizrak, D., H.M. Levitin, A.C. Delgado*, et al.*, *Single-Cell Analysis of Regional Differences in Adult V-SVZ Neural Stem Cell Lineages.* Cell Rep, 2019. **26**(2): p. 394-406.e5.
23. Cebrian-Silla, A., M.A. Nascimento, S.A. Redmond*, et al.*, *Single-cell analysis of the ventricular-subventricular zone reveals signatures of dorsal and ventral adult neurogenesis.* eLife, 2021. **10**: p. e67436.
24. Llorens-Bobadilla, E., S. Zhao, A. Baser*, et al.*, *Single-Cell Transcriptomics Reveals a Population of Dormant Neural Stem Cells that Become Activated upon Brain Injury.* Cell Stem Cell, 2015. **17**(3): p. 329-40.
25. Gerrits, E., N. Brouwer, S.M. Kooistra*, et al.*, *Distinct amyloid-β and tau-associated microglia profiles in Alzheimer's disease.* Acta Neuropathol, 2021. **141**(5): p. 681-696.
26. Zheng, G.X.Y., J.M. Terry, P. Belgrader*, et al.*, *Massively parallel digital transcriptional profiling of single cells.* Nature Communications, 2017. **8**(1): p. 14049.
27. Hao, Y., S. Hao, E. Andersen-Nissen*, et al.*, *Integrated analysis of multimodal single-cell data.* Cell, 2021. **184**(13): p. 3573-3587.e29.
28. Galili, T., A. O'Callaghan, J. Sidi*, et al.*, *heatmaply: an R package for creating interactive cluster heatmaps for online publishing.* Bioinformatics, 2018. **34**(9): p. 1600-1602.
29. Angerer, P., L. Haghverdi, M. Büttner*, et al.*, *destiny: diffusion maps for large-scale single-cell data in R.* Bioinformatics, 2016. **32**(8): p. 1241-1243.
30. Angerer, P., D.S. Fischer, F.J. Theis*, et al.*, *Automatic identification of relevant genes from low-dimensional embeddings of single-cell RNA-seq data.* Bioinformatics, 2020. **36**(15): p. 4291-4295.
31. Skene, N.G., J. Bryois, T.E. Bakken*, et al.*, *Genetic identification of brain cell types underlying schizophrenia.* Nature Genetics, 2018. **50**(6): p. 825-833.
32. de Leeuw, C.A., J.M. Mooij, T. Heskes*, et al.*, *MAGMA: generalized gene-set analysis of GWAS data.* PLoS Comput Biol, 2015. **11**(4): p. e1004219.
33. Skene, N.G. and S.G.N. Grant, *Identification of Vulnerable Cell Types in Major Brain Disorders Using Single Cell Transcriptomes and Expression Weighted Cell Type Enrichment.* Frontiers in Neuroscience, 2016. **10**.
34. *Biological insights from 108 schizophrenia-associated genetic loci.* Nature, 2014. **511**(7510): p. 421-7.
35. Stahl, E.A., G. Breen, A.J. Forstner*, et al.*, *Genome-wide association study identifies 30 loci associated with bipolar disorder.* Nature Genetics, 2019. **51**(5): p. 793-803.
36. Anney, R.J.L., S. Ripke, V. Anttila*, et al.*, *Meta-analysis of GWAS of over 16,000 individuals with autism spectrum disorder highlights a novel locus at 10q24.32 and a significant overlap with schizophrenia.* Molecular Autism, 2017. **8**(1): p. 21.
37. Liu, J.Z., S. van Sommeren, H. Huang*, et al.*, *Association analyses identify 38 susceptibility loci for inflammatory bowel disease and highlight shared genetic risk across populations.* Nat Genet, 2015. **47**(9): p. 979-986.
38. Finak, G., A. McDavid, M. Yajima*, et al.*, *MAST: a flexible statistical framework for assessing transcriptional changes and characterizing heterogeneity in single-cell RNA sequencing data.* Genome Biology, 2015. **16**(1): p. 278.
39. Bates, D., M. Mächler, B. Bolker*, et al.*, *Fitting Linear Mixed-Effects Models Using lme4.* Journal of Statistical Software, 2015. **67**(1): p. 1 - 48.
40. Newman, A.M., C.B. Steen, C.L. Liu*, et al.*, *Determining cell type abundance and expression from bulk tissues with digital cytometry.* Nature Biotechnology, 2019. **37**(7): p. 773-782.
41. Blomfield, I.M., B. Rocamonde, M.D.M. Masdeu*, et al.*, *Id4 promotes the elimination of the pro-activation factor Ascl1 to maintain quiescence of adult hippocampal stem cells.* Elife, 2019. **8**.
42. Zhang, R., M. Boareto, A. Engler*, et al.*, *Id4 Downstream of Notch2 Maintains Neural Stem Cell Quiescence in the Adult Hippocampus.* Cell Rep, 2019. **28**(6): p. 1485-1498.e6.
43. Episkopou, V., *SOX2 functions in adult neural stem cells.* Trends Neurosci, 2005. **28**(5): p. 219-21.
44. Quiroga, A.C., C.C. Stolt, R. Diez del Corral*, et al.*, *Sox5 controls dorsal progenitor and interneuron specification in the spinal cord.* Dev Neurobiol, 2015. **75**(5): p. 522-38.

45. Azim, E., D. Jabaudon, R.M. Fame*, et al.*, *SOX6 controls dorsal progenitor identity and interneuron diversity during neocortical development.* Nat Neurosci, 2009. **12**(10): p. 1238-47.
46. Batiuk, M.Y., A. Martirosyan, J. Wahis*, et al.*, *Identification of region-specific astrocyte subtypes at single cell resolution.* Nature Communications, 2020. **11**(1): p. 1220.
47. Manning, C.S., V. Biga, J. Boyd*, et al.*, *Quantitative single-cell live imaging links HES5 dynamics with cell-state and fate in murine neurogenesis.* Nature Communications, 2019. **10**(1): p. 2835.
48. Wang, H., G. Ge, Y. Uchida*, et al.*, *Gli3 is required for maintenance and fate specification of cortical progenitors.* J Neurosci, 2011. **31**(17): p. 6440-8.
49. Semerci, F., W.T.-S. Choi, A. Bajic*, et al.*, *Lunatic fringe-mediated Notch signaling regulates adult hippocampal neural stem cell maintenance.* eLife, 2017. **6**: p. e24660.
50. Kallur, T., R. Gisler, O. Lindvall*, et al.*, *Pax6 promotes neurogenesis in human neural stem cells.* Mol Cell Neurosci, 2008. **38**(4): p. 616-28.
51. Sansom, S.N., D.S. Griffiths, A. Faedo*, et al.*, *The level of the transcription factor Pax6 is essential for controlling the balance between neural stem cell self-renewal and neurogenesis.* PLoS Genet, 2009. **5**(6): p. e1000511.
52. Ortiz-Álvarez, G., M. Daclin, A. Shihavuddin*, et al.*, *Adult Neural Stem Cells and Multiciliated Ependymal Cells Share a Common Lineage Regulated by the Geminin Family Members.* Neuron, 2019. **102**(1): p. 159-172.e7.
53. Scott, C.E., S.L. Wynn, A. Sesay*, et al.*, *SOX9 induces and maintains neural stem cells.* Nat Neurosci, 2010. **13**(10): p. 1181-9.
54. Sim, F.J., C. Zhao, J. Penderis*, et al.*, *The age-related decrease in CNS remyelination efficiency is attributable to an impairment of both oligodendrocyte progenitor recruitment and differentiation.* J Neurosci, 2002. **22**(7): p. 2451-9.
55. Grubman, A., G. Chew, J.F. Ouyang*, et al.*, *A single-cell atlas of entorhinal cortex from individuals with Alzheimer's disease reveals cell-type-specific gene expression regulation.* Nat Neurosci, 2019. **22**(12): p. 2087-2097.
56. Dredge, B.K. and K.B. Jensen, *NeuN/Rbfox3 nuclear and cytoplasmic isoforms differentially regulate alternative splicing and nonsense-mediated decay of Rbfox2.* PLoS One, 2011. **6**(6): p. e21585.
57. Dulken, B.W., D.S. Leeman, S.C. Boutet*, et al.*, *Single-Cell Transcriptomic Analysis Defines Heterogeneity and Transcriptional Dynamics in the Adult Neural Stem Cell Lineage.* Cell Reports, 2017. **18**(3): p. 777-790.
58. Cochard, L.M., L.-C. Levros, S.E. Joppé*, et al.*, *Manipulation of EGFR-Induced Signaling for the Recruitment of Quiescent Neural Stem Cells in the Adult Mouse Forebrain.* Frontiers in Neuroscience, 2021. **15**.
59. Weickert, C.S. and M. Blum, *Striatal TGF-alpha: postnatal developmental expression and evidence for a role in the proliferation of subependymal cells.* Brain Res Dev Brain Res, 1995. **86**(1-2): p. 203-16.
60. Lui, J.H., T.J. Nowakowski, A.A. Pollen*, et al.*, *Radial glia require PDGFD-PDGFRβ signalling in human but not mouse neocortex.* Nature, 2014. **515**(7526): p. 264-8.
61. Arlotta, P., B.J. Molyneaux, D. Jabaudon*, et al.*, *Ctip2 Controls the Differentiation of Medium Spiny Neurons and the Establishment of the Cellular Architecture of the Striatum.* The Journal of Neuroscience, 2008. **28**(3): p. 622.
62. Kruusmägi, M., S. Zelenin, H. Brismar*, et al.*, *Intracellular dynamics of calcyon, a neuron-specific vesicular protein.* Neuroreport, 2007. **18**(15): p. 1547-51.
63. Artegiani, B., A. Lyubimova, M. Muraro*, et al.*, *A Single-Cell RNA Sequencing Study Reveals Cellular and Molecular Dynamics of the Hippocampal Neurogenic Niche.* Cell Rep, 2017. **21**(11): p. 3271-3284.
64. Vanlandewijck, M., L. He, M.A. Mäe*, et al.*, *A molecular atlas of cell types and zonation in the brain vasculature.* Nature, 2018. **554**(7693): p. 475-480.
65. Gerrits, E., N. Brouwer, S.M. Kooistra*, et al.*, *Distinct amyloid-β and tau-associated microglia profiles in Alzheimer's disease.* Acta Neuropathologica, 2021. **141**(5): p. 681-696.
66. Smith, X., A. Taylor and C.E. Rudd, *T-cell immune adaptor SKAP1 regulates the induction of collagen-induced arthritis in mice.* Immunol Lett, 2016. **176**: p. 122-7.

67. Alsema, A.M., Q. Jiang, L. Kracht*, et al.*, *Profiling Microglia From Alzheimer's Disease Donors and Non-demented Elderly in Acute Human Postmortem Cortical Tissue.* Frontiers in Molecular Neuroscience, 2020. **13**.
68. Lazarov, O. and R. Marr, *Of mice and men: neurogenesis, cognition and Alzheimer's disease.* Frontiers in Aging Neuroscience, 2013. **5**.
69. Sanai, N., A.D. Tramontin, A. Quiñones-Hinojosa*, et al.*, *Unique astrocyte ribbon in adult human brain contains neural stem cells but lacks chain migration.* Nature, 2004. **427**(6976): p. 740-744.
70. Millena, A.C., B.T. Vo and S.A. Khan, *JunD Is Required for Proliferation of Prostate Cancer Cells and Plays a Role in Transforming Growth Factor-β (TGF-β)-induced Inhibition of Cell Proliferation*.* Journal of Biological Chemistry, 2016. **291**(34): p. 17964-17976.
71. Elliott, B., A.C. Millena, L. Matyunina*, et al.*, *Essential role of JunD in cell proliferation is mediated via MYC signaling in prostate cancer cells.* Cancer Lett, 2019. **448**: p. 155-167.
72. Meixner, A., F. Karreth, L. Kenner*, et al.*, *JunD regulates lymphocyte proliferation and T helper cell cytokine expression.* The EMBO Journal, 2004. **23**(6): p. 1325-1335.
73. Morgan, D.J., S. Wei, I. Gomes*, et al.*, *The propeptide precursor proSAAS is involved in fetal neuropeptide processing and body weight regulation.* J Neurochem, 2010. **113**(5): p. 1275-84.
74. Al-Shammari, A.R., S.K. Bhardwaj, K. Musaelyan*, et al.*, *Schizophrenia-related dysbindin-1 gene is required for innate immune response and homeostasis in the developing subventricular zone.* NPJ Schizophr, 2018. **4**(1): p. 15.
75. Wegiel, J., I. Kuchna, K. Nowicki*, et al.*, *The neuropathology of autism: defects of neurogenesis and neuronal migration, and dysplastic changes.* Acta Neuropathologica, 2010. **119**(6): p. 755-770.
76. Shimogori, T., J. VanSant, E. Paik*, et al.*, *Members of the Wnt, Fz, and Frp gene families expressed in postnatal mouse cerebral cortex.* J Comp Neurol, 2004. **473**(4): p. 496-510.
77. Sorrells, S.F., M.F. Paredes, A. Cebrian-Silla*, et al.*, *Human hippocampal neurogenesis drops sharply in children to undetectable levels in adults.* Nature, 2018. **555**(7696): p. 377-381.
78. Weissleder, C., S.J. Fung, M.W. Wong*, et al.*, *Decline in Proliferation and Immature Neuron Markers in the Human Subependymal Zone during Aging: Relationship to EGF- and FGF-Related Transcripts.* Front Aging Neurosci, 2016. **8**: p. 274.
79. Borrett, M.J., B.T. Innes, D. Jeong*, et al.*, *Single-Cell Profiling Shows Murine Forebrain Neural Stem Cells Reacquire a Developmental State when Activated for Adult Neurogenesis.* Cell Reports, 2020. **32**(6): p. 108022.
80. Boudesco, C., S. Cause, G. Jego*, et al.*, *Hsp70: A Cancer Target Inside and Outside the Cell.* Methods Mol Biol, 2018. **1709**: p. 371-396.
81. Zhao, N., J. Zhang, L. Zhao*, et al.*, *Long Noncoding RNA NONHSAT079852.2 Contributes to GBM Recurrence by Functioning as a ceRNA for has-mir-10401-3p to Facilitate HSPA1A Upregulation.* Front Oncol, 2021. **11**: p. 636632.
82. Bergmann, O., J. Liebl, S. Bernard*, et al.*, *The Age of Olfactory Bulb Neurons in Humans.* Neuron, 2012. **74**(4): p. 634-639.
83. Coletti, A.M., D. Singh, S. Kumar*, et al.*, *Characterization of the ventricular-subventricular stem cell niche during human brain development.* Development, 2018. **145**(20): p. dev170100.
84. Kalamakis, G., D. Brüne, S. Ravichandran*, et al.*, *Quiescence Modulates Stem Cell Maintenance and Regenerative Capacity in the Aging Brain.* Cell, 2019. **176**(6): p. 1407-1419.e14.
85. Solano Fonseca, R., S. Mahesula, D.M. Apple*, et al.*, *Neurogenic Niche Microglia Undergo Positional Remodeling and Progressive Activation Contributing to Age-Associated Reductions in Neurogenesis.* Stem Cells Dev, 2016. **25**(7): p. 542-55.
86. Li, N., S.W. Teng, L. Zhao*, et al.*, *Carboxypeptidase E Regulates Activity-Dependent TrkB Neuronal Surface Insertion and Hippocampal Memory.* J Neurosci, 2021. **41**(33): p. 6987-7002.

87. Woronowicz, A., H. Koshimizu, S.Y. Chang*, et al.*, *Absence of carboxypeptidase E leads to adult hippocampal neuronal degeneration and memory deficits.* Hippocampus, 2008. **18**(10): p. 1051-63.
88. Wisdom, N.M., J. Mignogna and R.L. Collins, *Variability in Wechsler Adult Intelligence Scale-IV subtest performance across age.* Arch Clin Neuropsychol, 2012. **27**(4): p. 389-97.
89. Fabbri, C., G.M. Leggio, F. Drago*, et al.*, *Imputed expression of schizophrenia-associated genes and cognitive measures in patients with schizophrenia.* Mol Genet Genomic Med, 2022. **10**(6): p. e1942.
90. Wang, X., K.B. Hu, Y.Q. Zhang*, et al.*, *Comprehensive analysis of aberrantly expressed profiles of lncRNAs, miRNAs and mRNAs with associated ceRNA network in cholangiocarcinoma.* Cancer Biomark, 2018. **23**(4): p. 549-559.
91. Salvadores, N., M. Sanhueza, P. Manque*, et al.*, *Axonal Degeneration during Aging and Its Functional Role in Neurodegenerative Disorders.* Front Neurosci, 2017. **11**: p. 451.
92. Ueno, M., Y. Nakamura, H. Nakagawa*, et al.*, *Olig2-Induced Semaphorin Expression Drives Corticospinal Axon Retraction After Spinal Cord Injury.* Cereb Cortex, 2020. **30**(11): p. 5702-5716.
93. Liu, H., L. Wang, Z. Geng*, et al.*, *A voxel-based morphometric study of age- and sex-related changes in white matter volume in the normal aging brain.* Neuropsychiatr Dis Treat, 2016. **12**: p. 453-65.
94. Coelho, A., H.M. Fernandes, R. Magalhães*, et al.*, *Signatures of white-matter microstructure degradation during aging and its association with cognitive status.* Scientific Reports, 2021. **11**(1): p. 4517.
95. Tutuncu, M., J. Tang, N.A. Zeid*, et al.*, *Onset of progressive phase is an age-dependent clinical milestone in multiple sclerosis.* Multiple Sclerosis Journal, 2012. **19**(2): p. 188-198.
96. Nait-Oumesmar, B., N. Picard-Riera, C. Kerninon*, et al.*, *Activation of the subventricular zone in multiple sclerosis: Evidence for early glial progenitors.* Proceedings of the National Academy of Sciences, 2007. **104**(11): p. 4694-4699.
97. Sankowski, R., C. Böttcher, T. Masuda*, et al.*, *Mapping microglia states in the human brain through the integration of high-dimensional techniques.* Nature Neuroscience, 2019. **22**(12): p. 2098-2110.
98. Olah, M., E. Patrick, A.C. Villani*, et al.*, *A transcriptomic atlas of aged human microglia.* Nat Commun, 2018. **9**(1): p. 539.
99. Galatro, T.F., I.R. Holtman, A.M. Lerario*, et al.*, *Transcriptomic analysis of purified human cortical microglia reveals age-associated changes.* Nature Neuroscience, 2017. **20**(8): p. 1162-1171.
100. Lim, D.A. and A. Alvarez-Buylla, *The Adult Ventricular-Subventricular Zone (V-SVZ) and Olfactory Bulb (OB) Neurogenesis.* Cold Spring Harb Perspect Biol, 2016. **8**(5).